Electronic Supplementary Material (ESI) for Materials Advances.

Relation among Absorbance Shifts, Mineralization Morphology, and Electronic Conductivity of π-Peptide Aggregates with Different Amino Acid Residues

Table of Contents

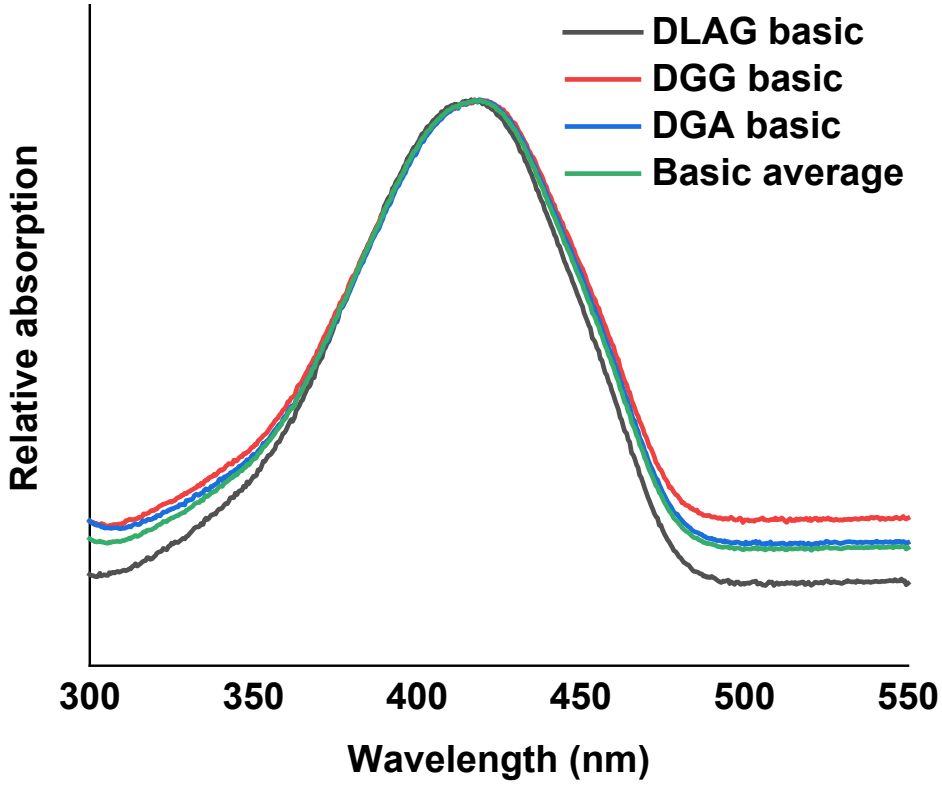

Figure S1. UV-vis absorption spectra for DGG-4T, DGA-4T, and DLAG-4T and their averages in basic medium after adding 15 μL of 1M KOH.

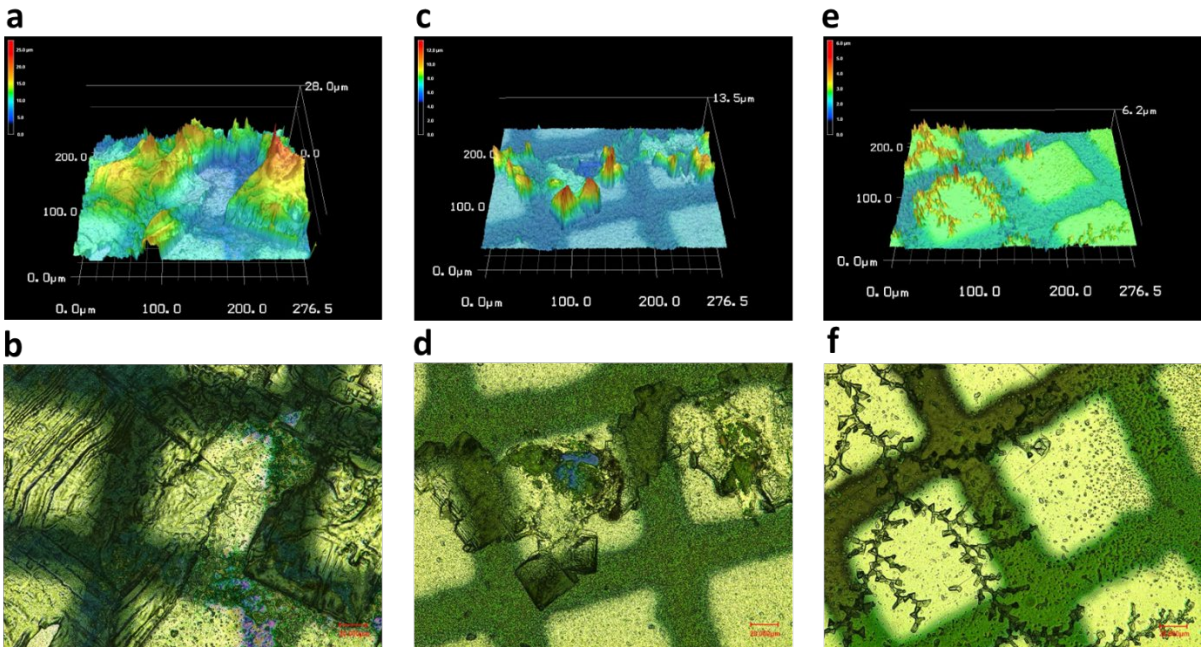

Figure S2. 3D height profile from laser optical microscopy scan of **(a)** DGG-4T with KCl at 50x magnification and its corresponding **(b)** 50x laser optical microscope image. 3D height profile from laser optical microscopy scan of **(c)** DGA-4T with KCl at 50x magnification and its corresponding **(d)** 50x laser optical microscope image. 3D height profile from laser optical microscopy scan of **(e)** DLAG-4T with KCl at 50x magnification and its corresponding **(f)** 50x laser optical microscope image.

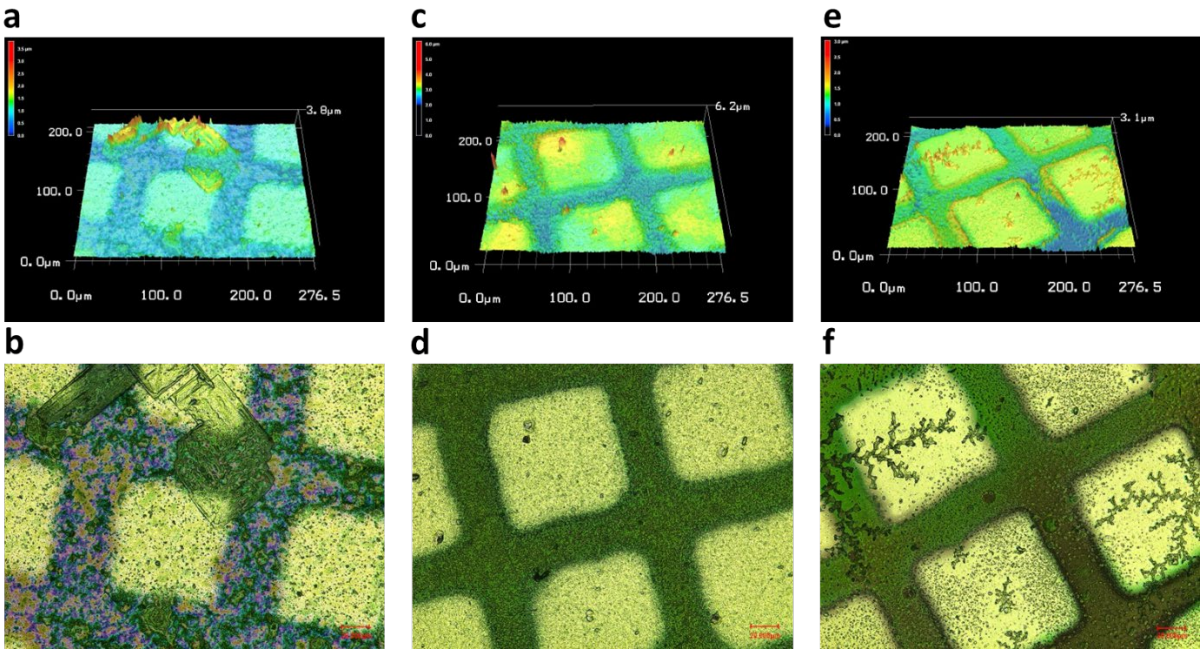

Figure S3. 3D height profile from laser optical microscopy scan of **(a)** DGG-4T without KCl at 50x magnification and its corresponding **(b)** 50x laser optical microscope image. 3D height profile from laser optical microscopy scan of **(c)** DGA-4T without KCl at 50x magnification and its corresponding **(d)** 50x laser optical microscope image. 3D height profile from laser

optical microscopy scan of **(e)** DLAG-4T without KCl at 50x magnification and its corresponding **(f)** 50x laser optical microscope image.

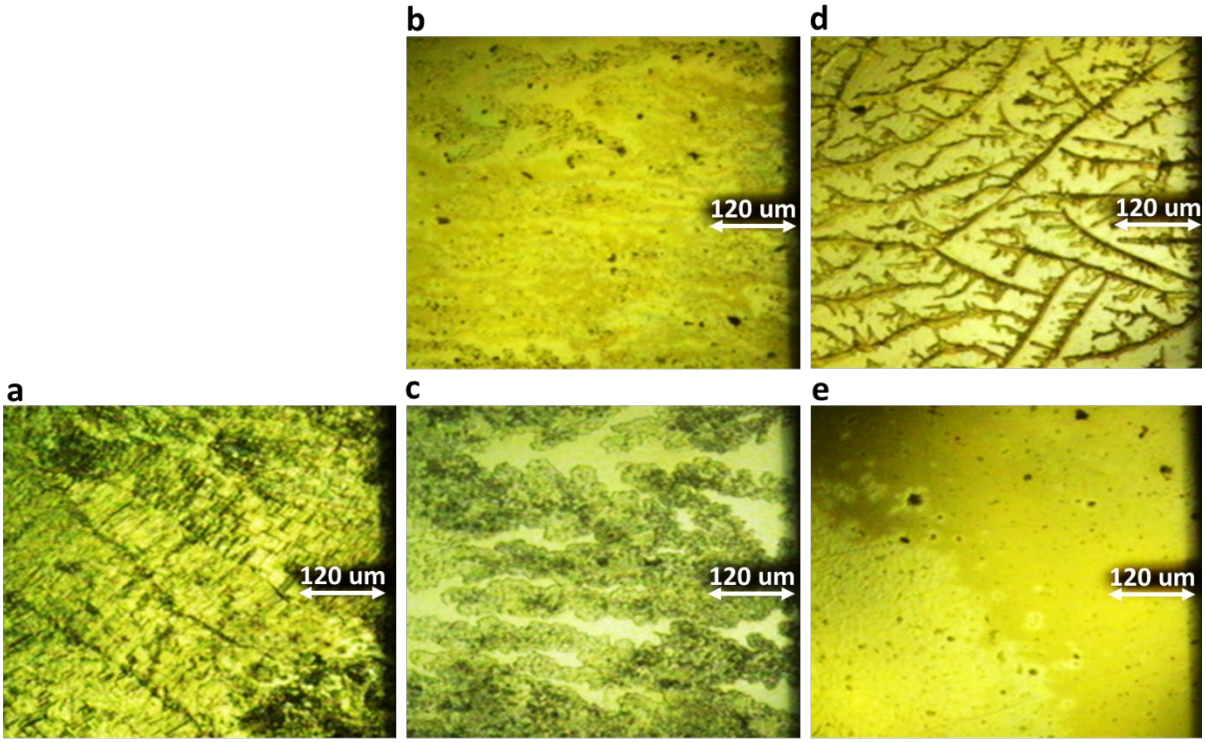

Figure S4. AFM images for **(a)** DGG-4T, **(b)** center of DGG-4T, **(c)** edge of DGG-4T, **(d)** center of DLAG-4T, and **(e)** edge of DLAG-4T.

a

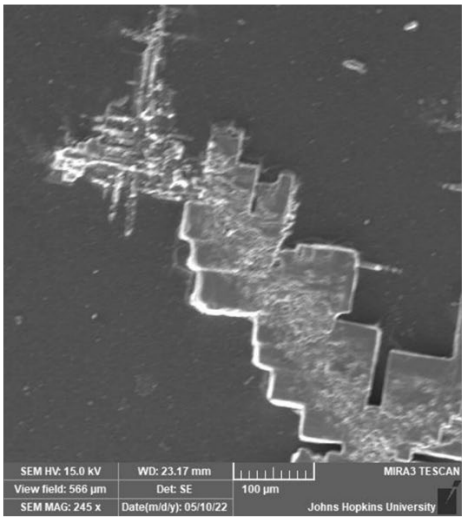

c

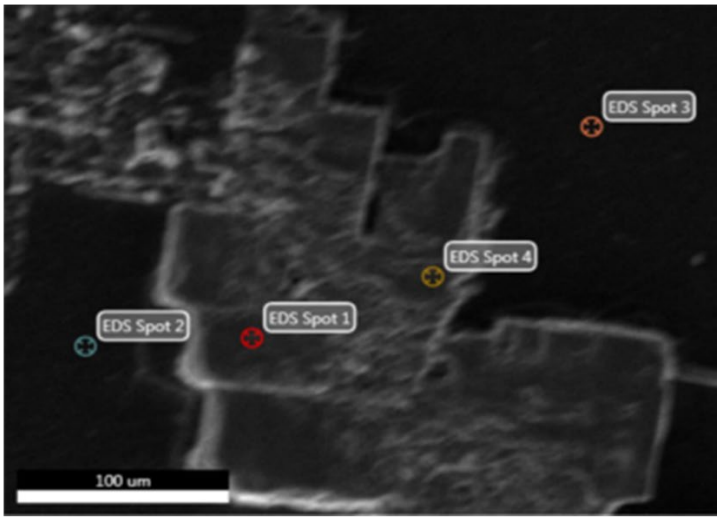

b

	Spot 1	Spot 2	Spot 3	Spot 4
Element	**Atomic %**	**Atomic %**	**Atomic %**	**Atomic %**
C K	0.02	37.59	37.31	0.03
O K	5.71	18	17.08	5.25
Si K	0.96	39.66	38.82	0.96
S K	1.3	3.1	3.24	1.27
Cl K	45.47	0.26	1.15	45.88
K K	44.63	0.62	1.42	45.14
Cr K	1.92	0.76	0.97	1.47

Figure S5. **(a)** SEM scan of DGG-4T at 245x magnification, **(b)** quantitative elemental composition analysis by SEM of EDS spots identified in (c), and **(c)** EDS scans from SEM for spots 1, 2, 3, and 4.

a

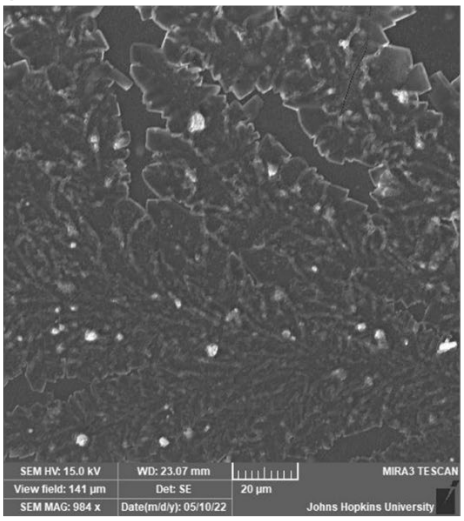

c

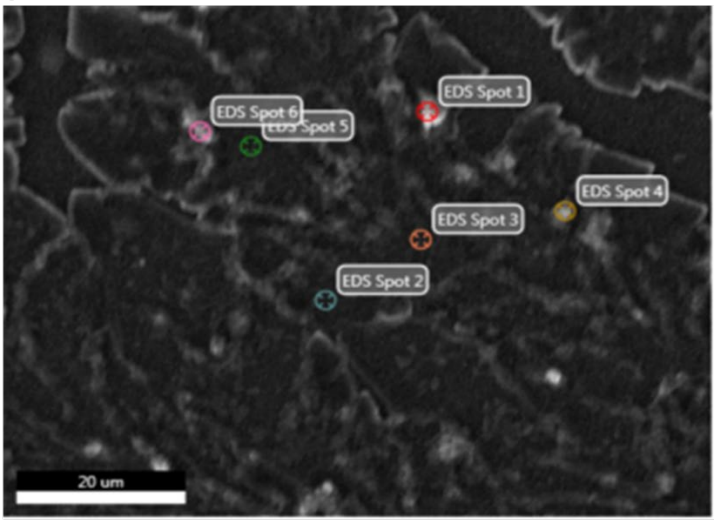

b

	Spot 1	Spot 2	Spot 3	Spot 4	Spot 5	Spot 6
Element	Atomic %	Atomic %	Atomic %	Atomic %	Atomic %	Atomic %
C K	3.09	36.9	38.79	9.87	41.09	0.76
O K	11.91	16.25	14.99	15.69	11.76	13.47
Si K	6.24	35.8	29.78	11.76	32.24	8.86
S K	5.31	7.26	6.92	7.15	9.61	7.08
Cl K	34.36	0.61	3.2	24.69	0.97	31.79
K K	36.61	1.75	4.82	27.39	2.62	35.17
Cr K	2.48	1.43	1.5	3.44	1.7	2.88

Figure S6. **(a)** SEM scan of DGG-4T at 984x magnification, **(b)** quantitative elemental composition analysis by SEM of EDS spots identified in (c), and **(c)** EDS scans from SEM for spots 1, 2, 3, 4, 5, and 6.

a

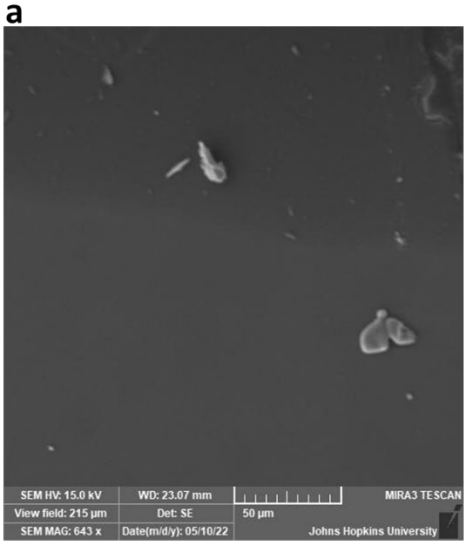

c

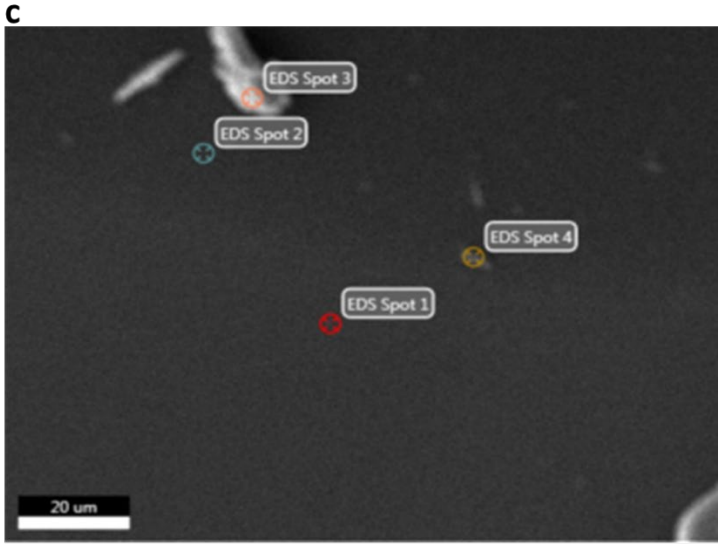

b

	Spot 1	Spot 2	Spot 3	Spot 4
Element	**Atomic %**	**Atomic %**	**Atomic %**	**Atomic %**
C K	13.53	35.58	22.81	31.1
O K	20.41	16.68	7.2	24.82
Si K	64.81	45.33	68.45	41.16
S K	0.15	1.26	0.69	1.22
Cl K	0.05	0.09	0.1	0.21
K K	0.04	0.2	0.12	0.3
Cr K	1.01	0.86	0.63	1.18

Figure S7. **(a)** SEM scan of DGG-4T at 643x magnification, **(b)** quantitative elemental composition analysis by SEM of EDS spots identified in (c), **(c)** EDS scans from SEM for spots 1, 2, 3, and 4.

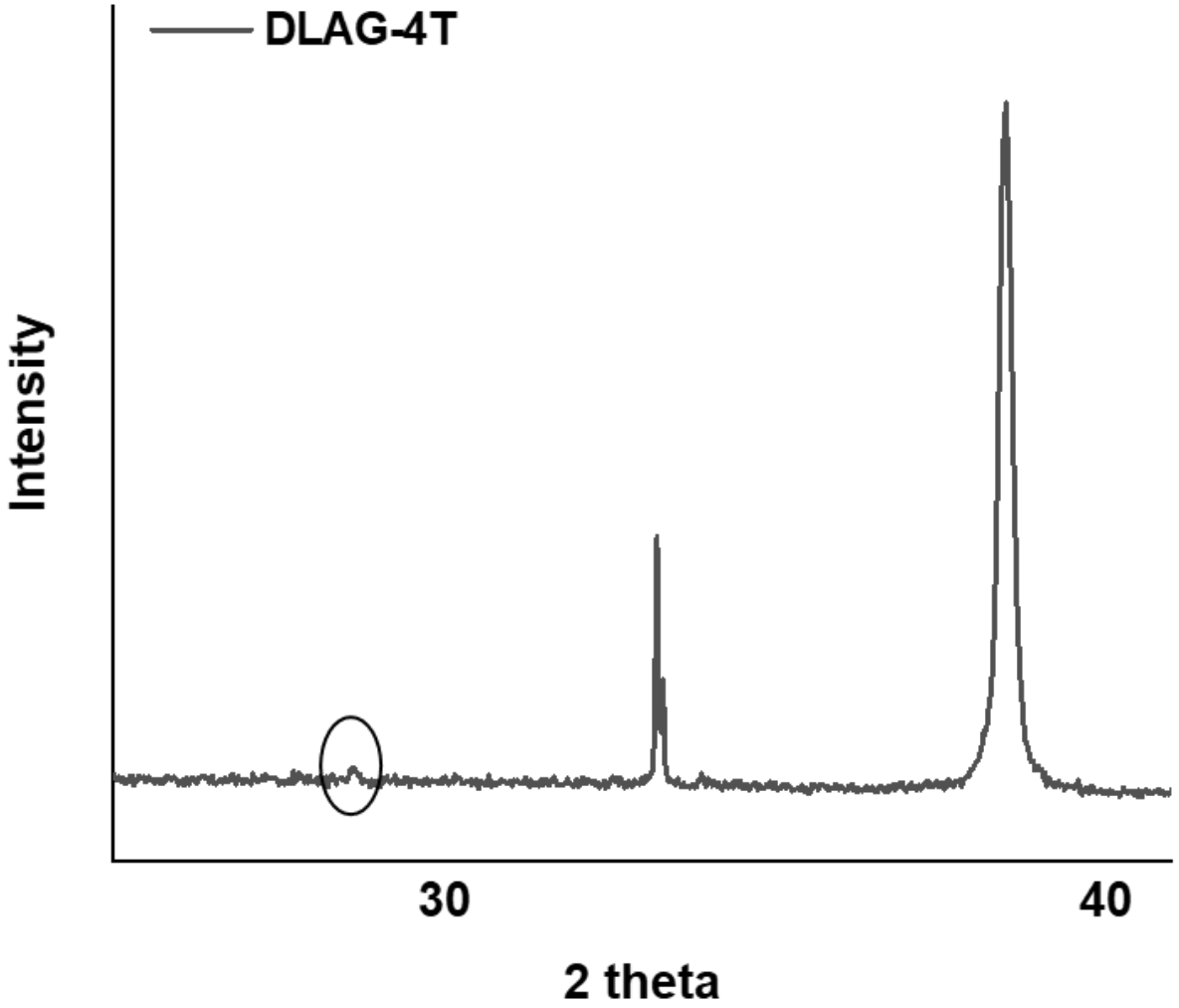

Figure S8. Zoomed in XRD graph of DLAG from **figure 6.** Showing the small KCl XRD peak in DLAG-4T due to less formation of bulk KCl crystals resulting in less KCl crystal planes diffracting X-ray beams from XRD.

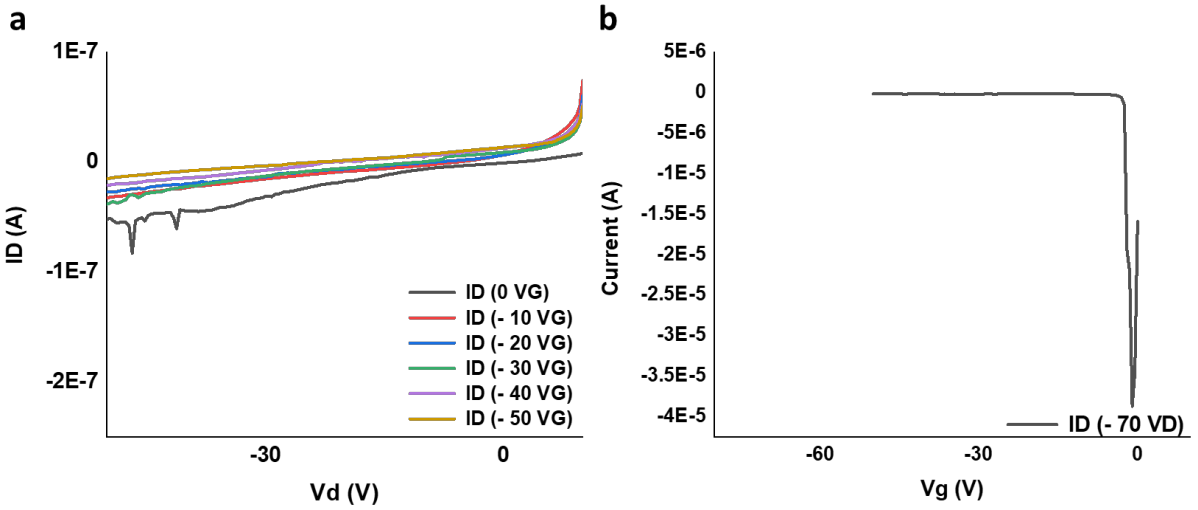

Figure S9. **(a)** Transfer curves of DGG-4T OFET measurements showing no semiconducting properties and **(b)** output curve of DGG-4T OFET measurement showing no semiconducting properties.

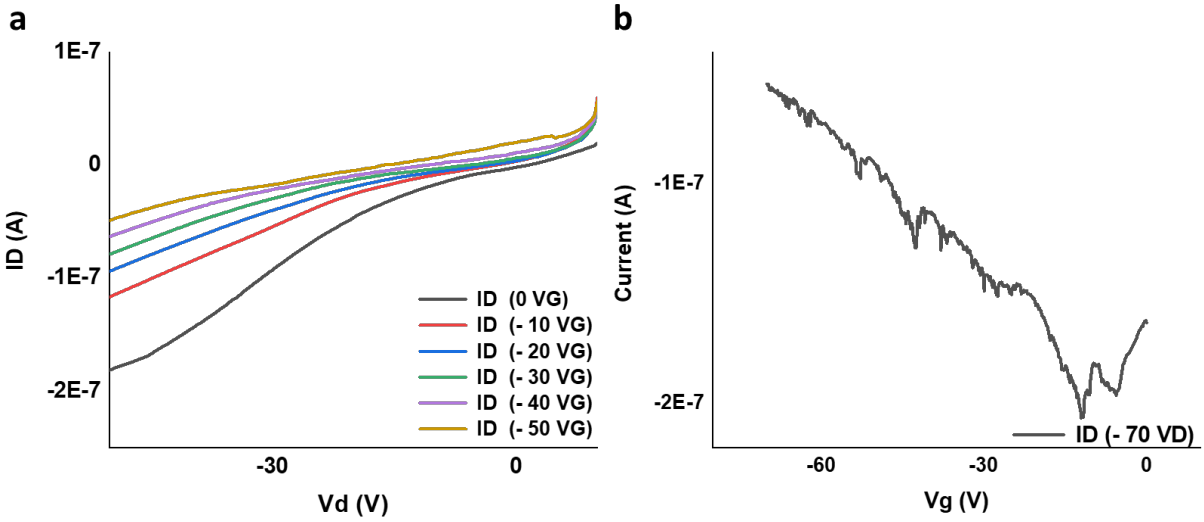

Figure S10. **(a)** Transfer curves of DGA-4T OFET measurements showing no semiconducting properties and **(b)** output curve of DGA-4T OFET measurement showing no semiconducting properties.

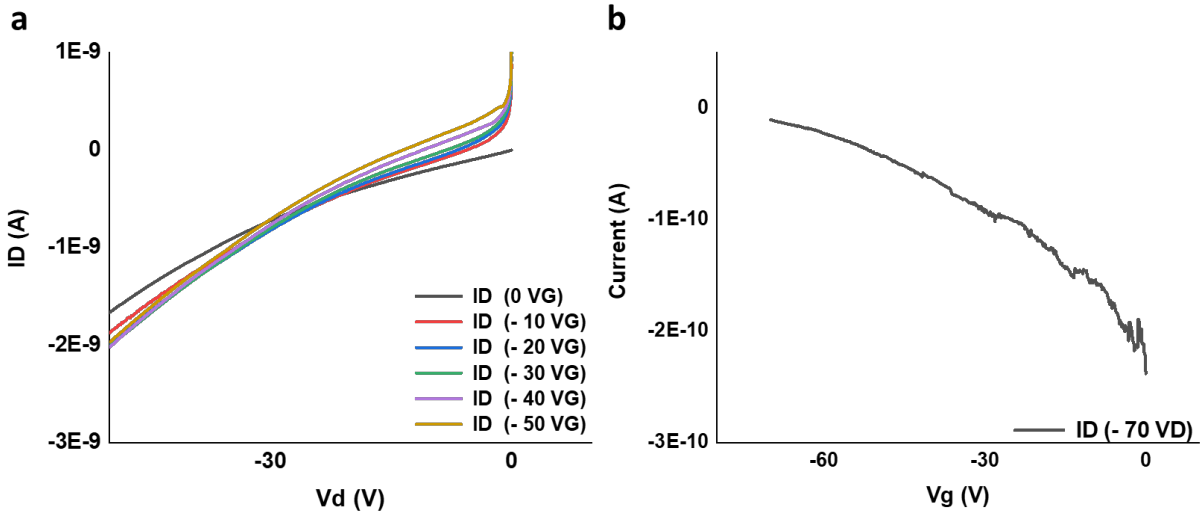

Figure S11. **(a)** Transfer curves of DLAG-4T OFET measurements showing no semiconducting properties and **(b)** output curve of DLAG-4T OFET measurement showing no semiconducting properties.

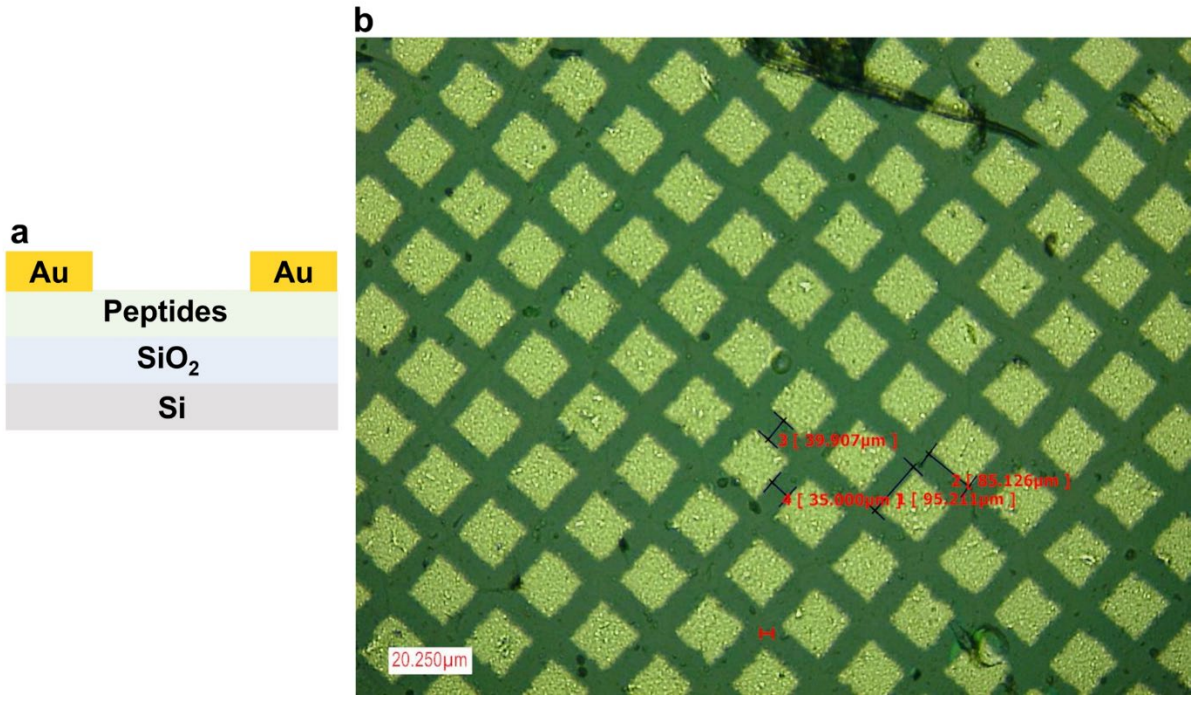

Figure S12. **(a)** OFET device structure of all OFET measurements for **figure S7-10. (b)** Laser optical microscope image of dimensions on the surface of OFET device after thermally evaporating 50 nm of gold electrode using a TEM grid mask.

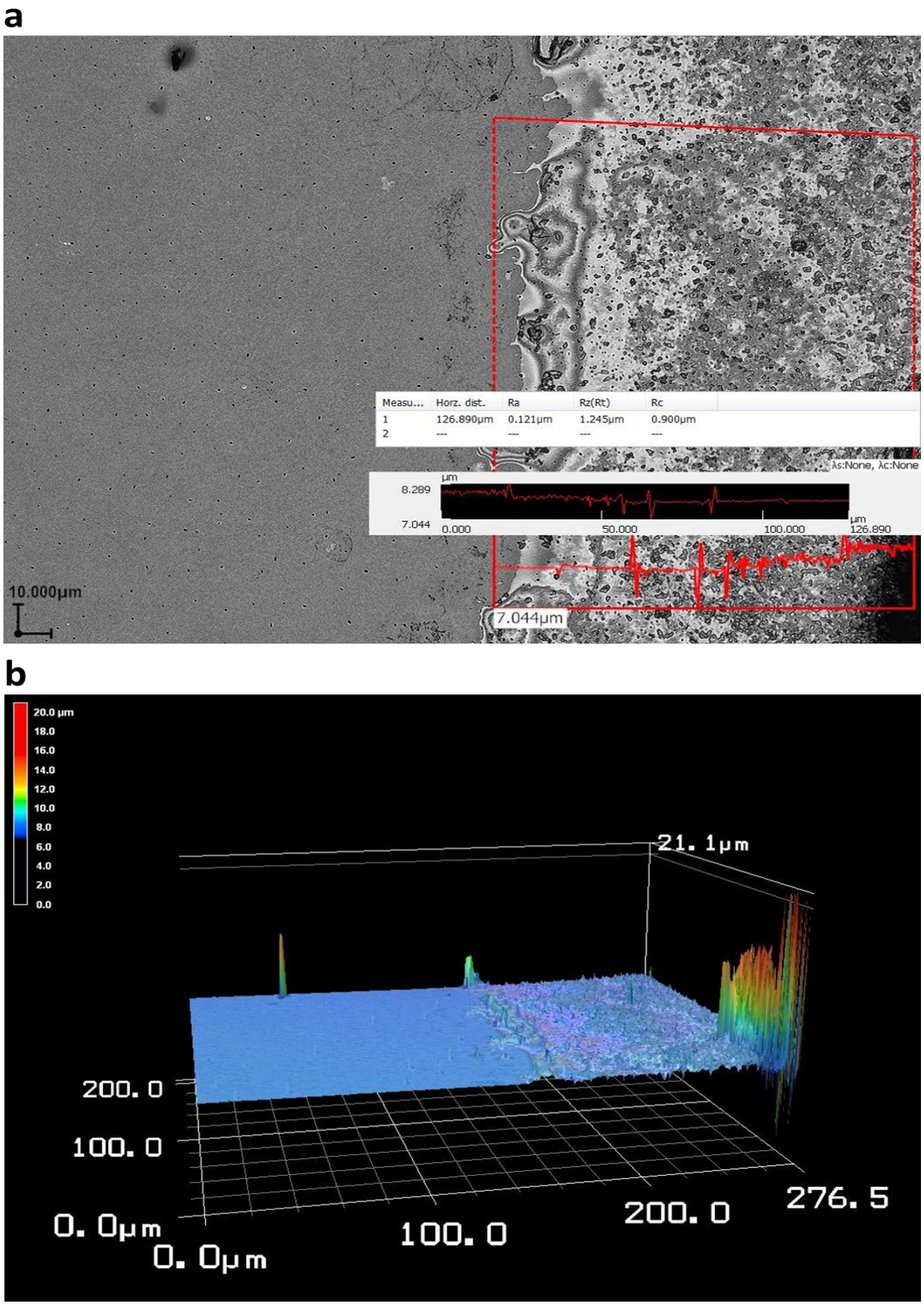

Figure S13. **(a)** Surface roughness profiling of laser scanned region at the edge of DGG-4T thin film on Si substrate and **(b)** 3D height profile image of same area for thickness.

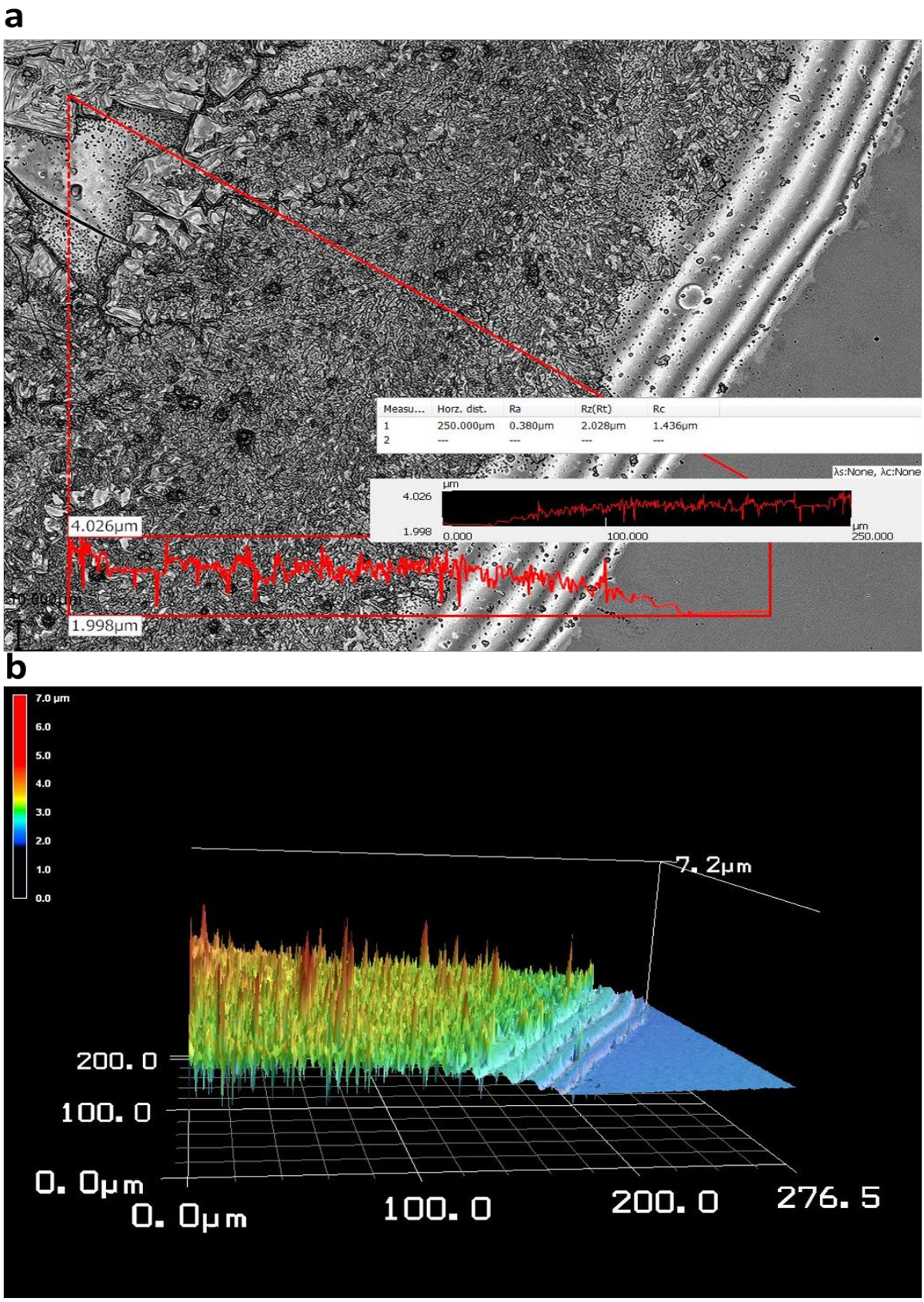

Figure S14. **(a)** Surface roughness profiling of laser scanned region at the edge of DGA-4T thin film on Si substrate and **(b)** 3D height profile image of same area for thickness.

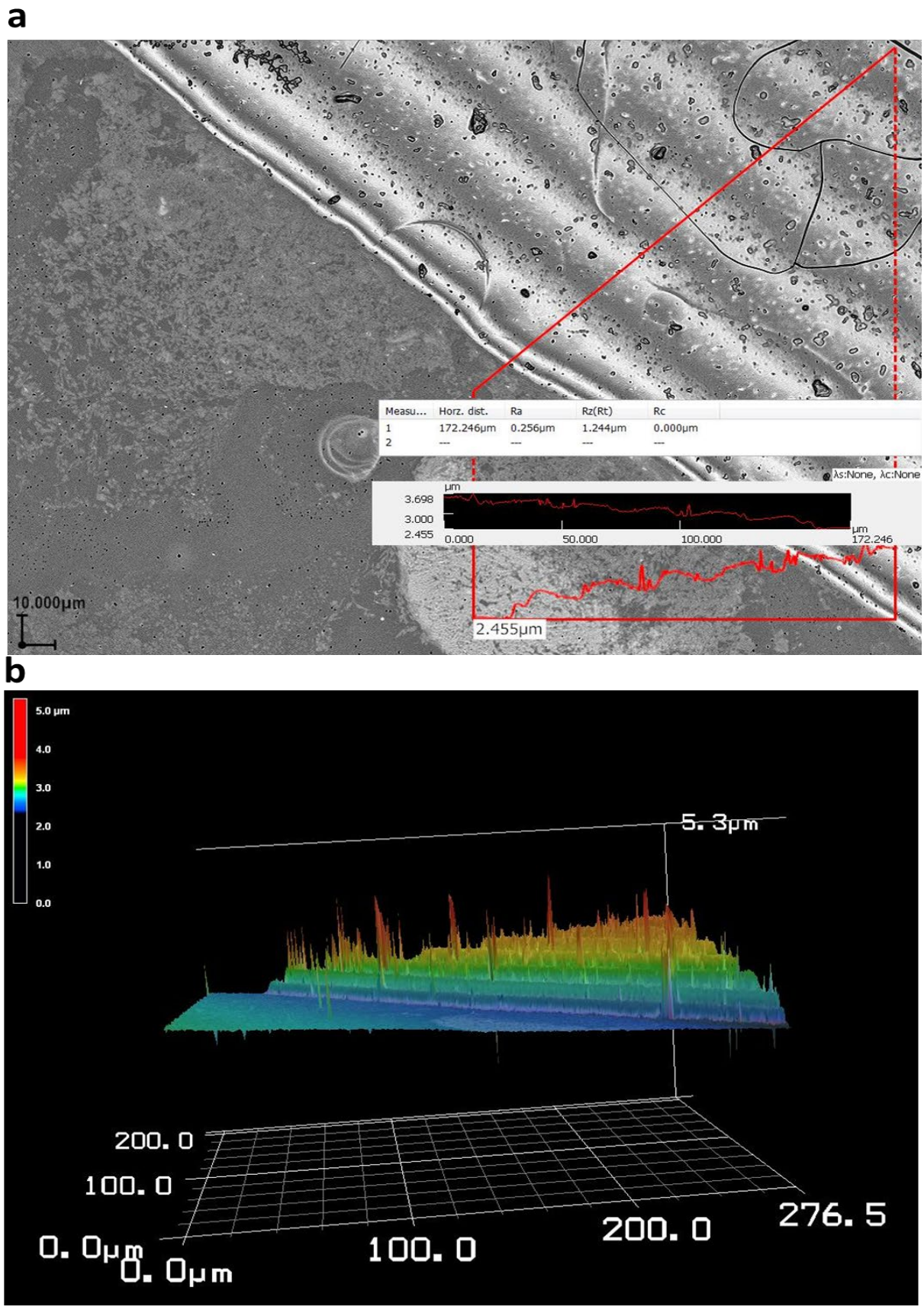

Figure S15. **(a)** Surface roughness profiling of laser scanned region at the edge of DLAG-4T thin film on Si substrate and **(b)** 3D height profile image of same area for thickness.

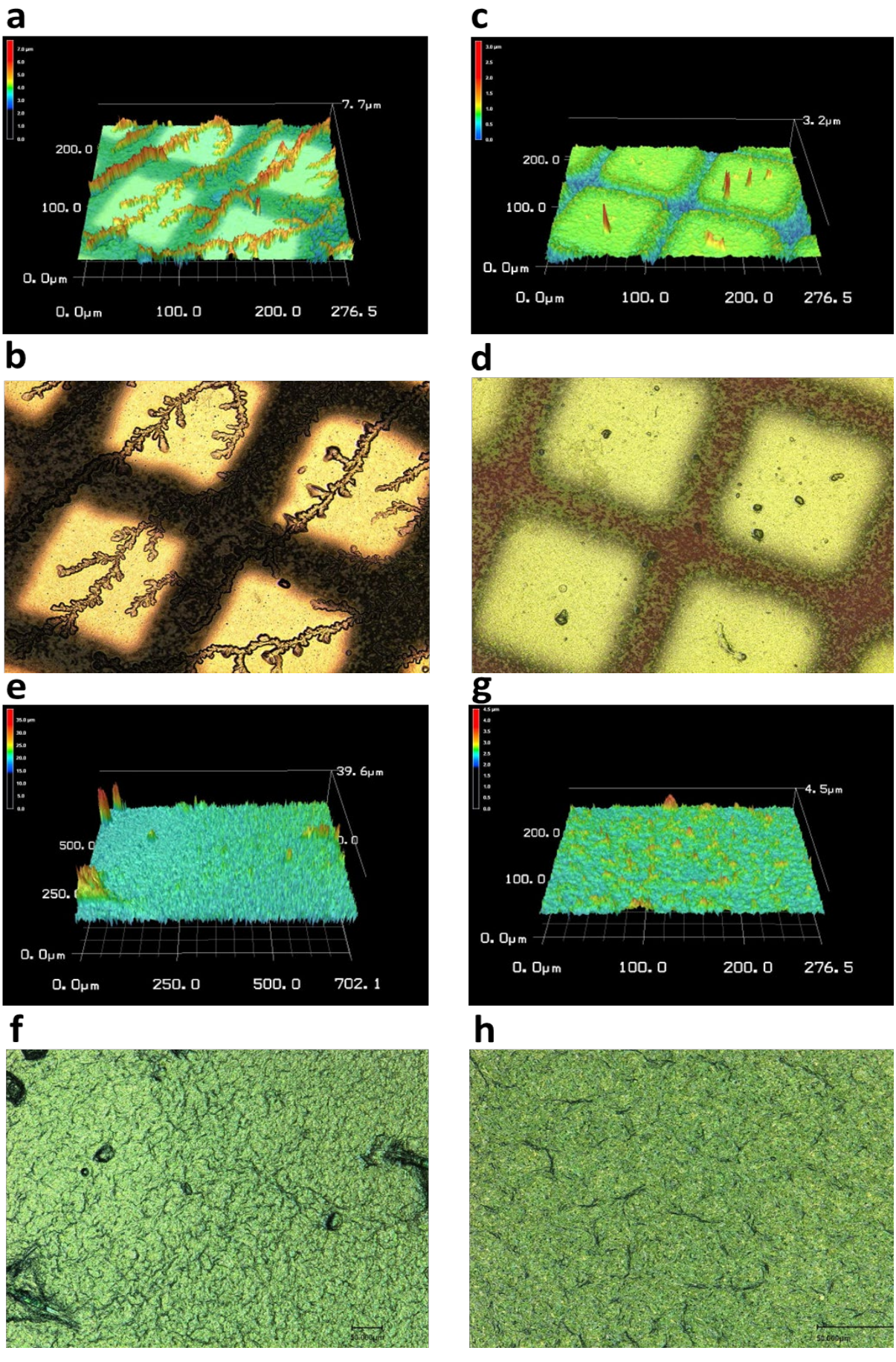
a
7. 7µm
200. 0
100. 0
0. 0µm
0. 0µm
100. 0
200. 0
276. 5
c
3. 2µm
200. 0
100. 0
0. 0µm
0. 0µm
100. 0
200. 0
276. 5
b
d
e
39. 6µm
500. 0
250.
0. 0µm
0. 0µm
250. 0
500. 0
702. 1
g
4. 5µm
200. 0
100. 0
0. 0µm
0. 0µm
100. 0
200. 0
276. 5
f
h

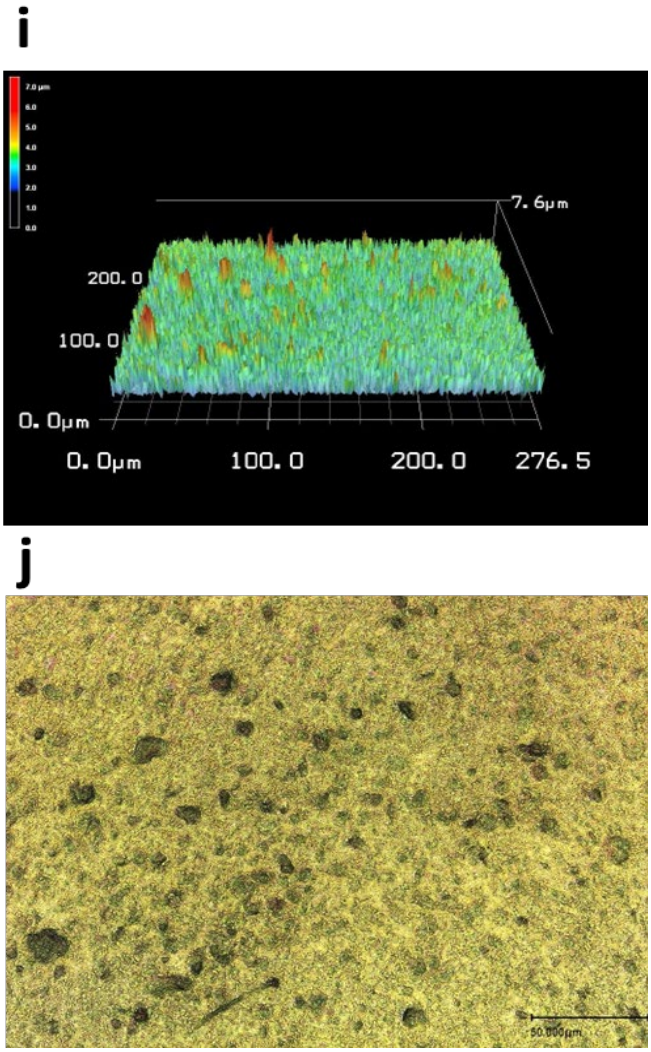

Figure S16. 3D height profile from laser optical microscopy scan of **(a)** VEVAG-PDI with KCl at 50x magnification and its corresponding **(b)** 50x laser optical microscope image. 3D height profile from laser optical microscopy scan of **(c)** VEVAA-PDI at 50x magnification and its corresponding **(d)** 50x laser optical microscope image. 3D height profile from laser optical microscopy scan of **(e)** DVAG-PDI without KCl at 50x magnification and its corresponding **(f)** 50x laser optical microscope image. 3D height profile from laser optical microscopy scan of **(g)** DVAG-PDI with KCl at 50x magnification and its corresponding **(h)** 50x laser optical microscope image. 3D height profile from laser optical microscopy scan of **(i)** DAIA-PDI at 50x magnification and its corresponding **(j)** 50x laser optical microscope image.

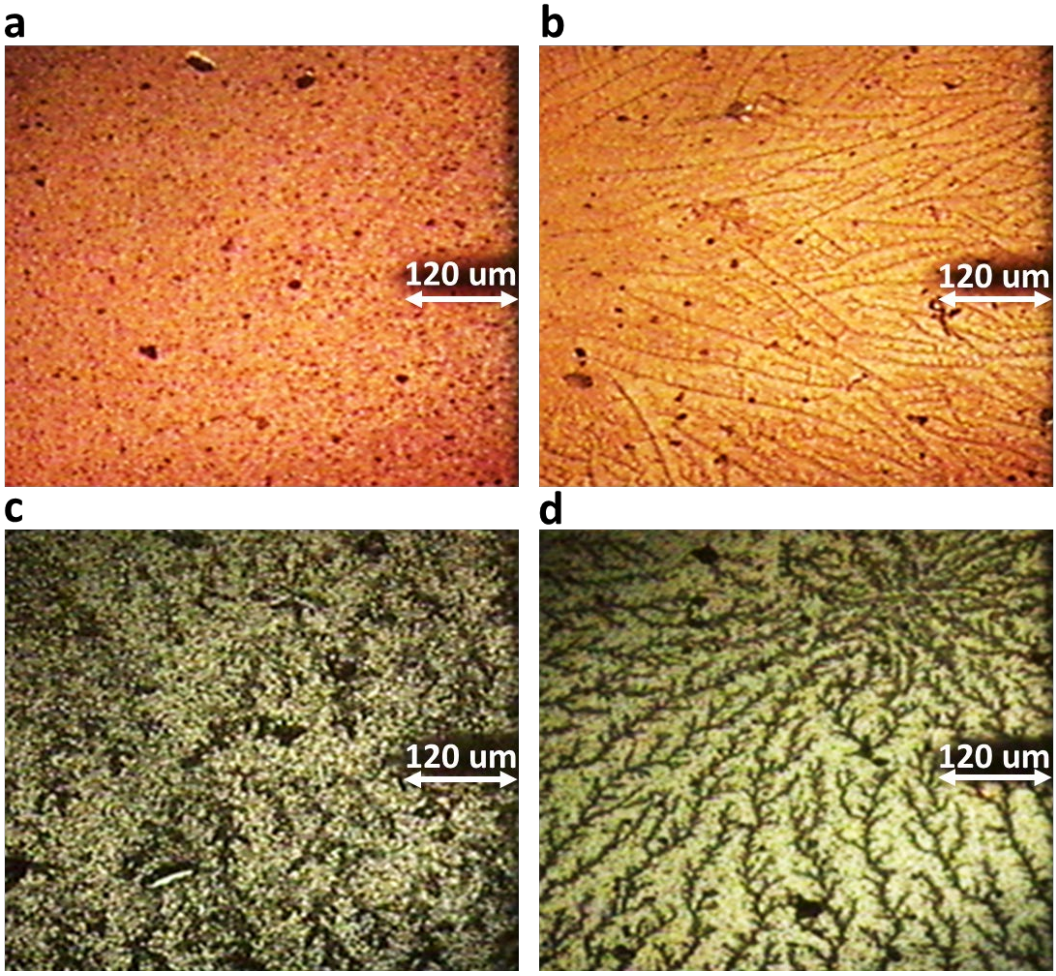

Figure S17. AFM images for **(a)** DAIA-PDI, **(b)** DVAG-PDI, **(c)** VEVAA-PDI, and **(d)** VEVAG-PDI.

a

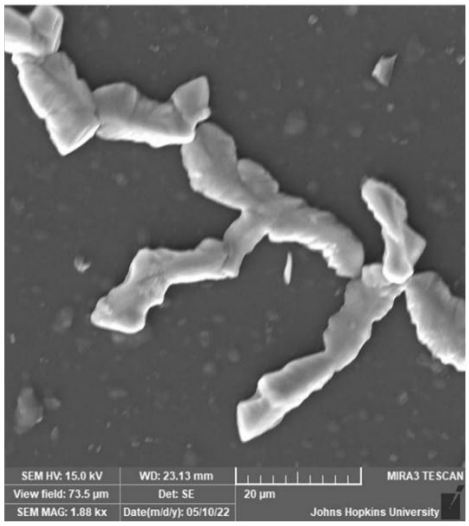

c

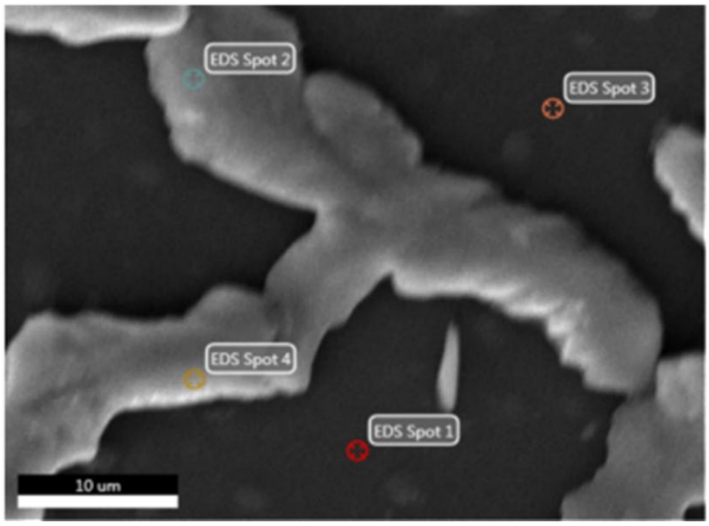

b

	Spot 1	Spot 2	Spot 3	Spot 4
Element	Atomic %	Atomic %	Atomic %	Atomic %
C K	40.69	0.03	36.66	2.17
O K	15.61	8.93	16.29	13
Si K	42.2	2.35	45.22	2.09
Cl K	0.38	43.36	0.47	39.62
K K	0.31	43.5	0.39	41.13
Cr K	0.8	1.83	0.96	1.99

Figure S18. **(a)** SEM scan of VEVAG-PDI at 1.88kx magnification, **(b)** quantitative elemental composition analysis by SEM of EDS spots identified in (c), **(c)** EDS scans from SEM for spots 1, 2, 3, and 4.

a

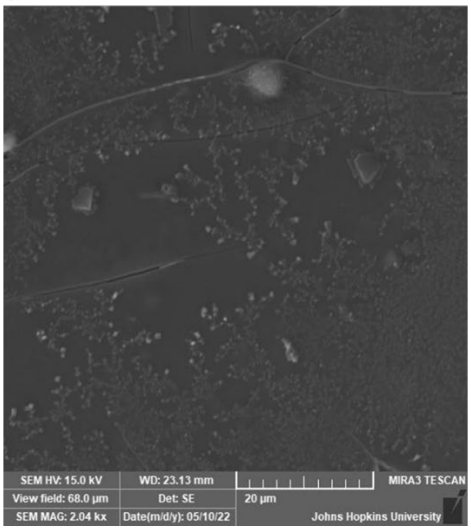

c

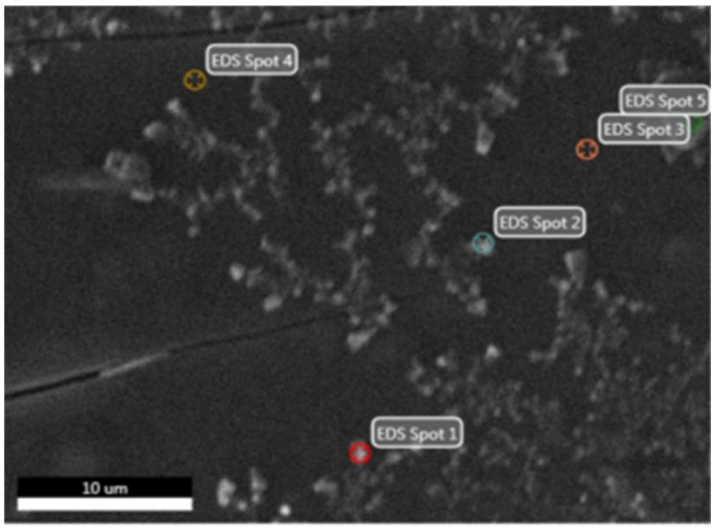

b

	Spot 1	Spot 2	Spot 3	Spot 4	Spot 5
Element	Atomic %	Atomic %	Atomic %	Atomic %	Atomic %
C K	39.47	33.78	41.4	43.18	25.25
O K	13.85	13.01	14.25	14.11	12.39
Si K	40.54	48.94	42.95	41.4	45.7
Cl K	2.36	1.58	0.34	0.38	8
K K	2.54	1.65	0.25	0.2	7.37
Cr K	1.23	1.04	0.8	0.73	1.3

Figure S19. **(a)** SEM scan of VEVAA-PDI at 2.04kx magnification, **(b)** quantitative elemental composition analysis by SEM of EDS spots identified in (c), **(c)** EDS scans from SEM for spots 1, 2, 3, 4, and 5.

a

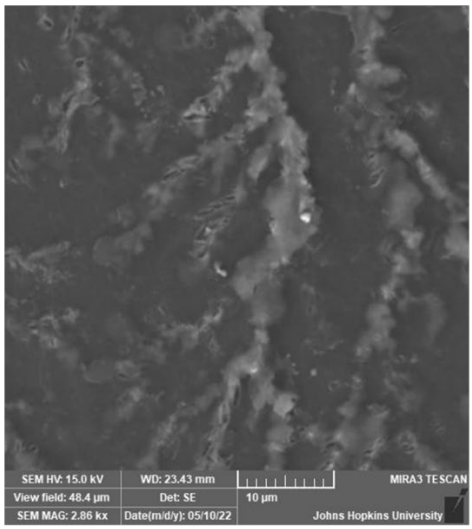

c

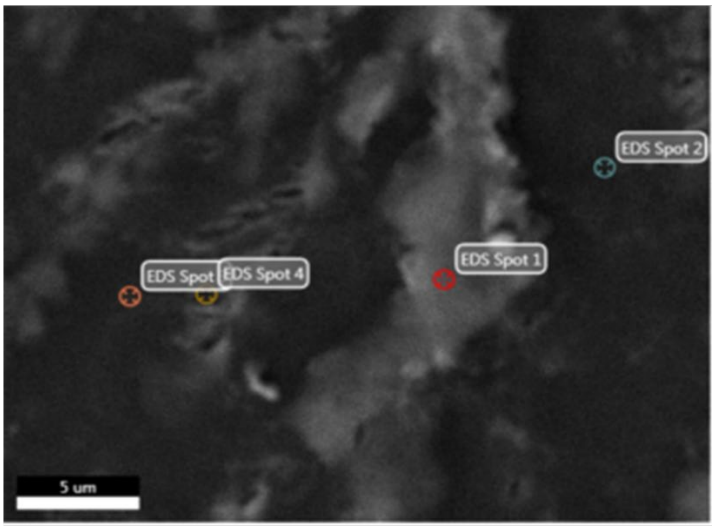

b

	Spot 1	Spot 2	Spot 3	Spot 4
Element	Atomic %	Atomic %	Atomic %	Atomic %
C K	18.46	29.24	30.28	28.2
O K	16.97	15.79	18.65	15.06
Si K	21.1	53.58	49.76	55.14
Cl K	20.89	0.27	0.31	0.43
K K	21.54	0.38	0.35	0.45
Cr K	1.04	0.74	0.64	0.71

Figure S20. **(a)** SEM scan of DAVG-PDI at 2.86kx magnification, **(b)** quantitative elemental composition analysis by SEM of EDS spots identified in (c), **(c)** EDS scans from SEM for spots 1, 2, 3, and 4.

a

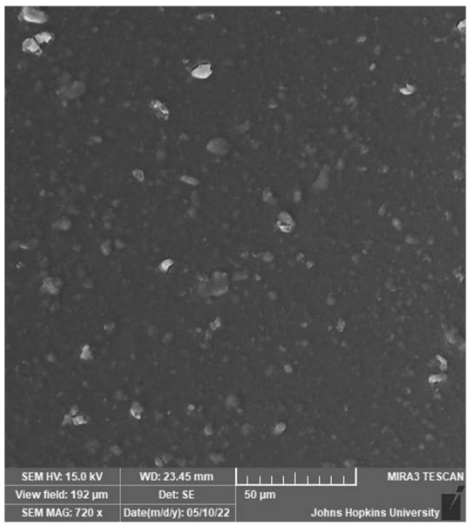

c

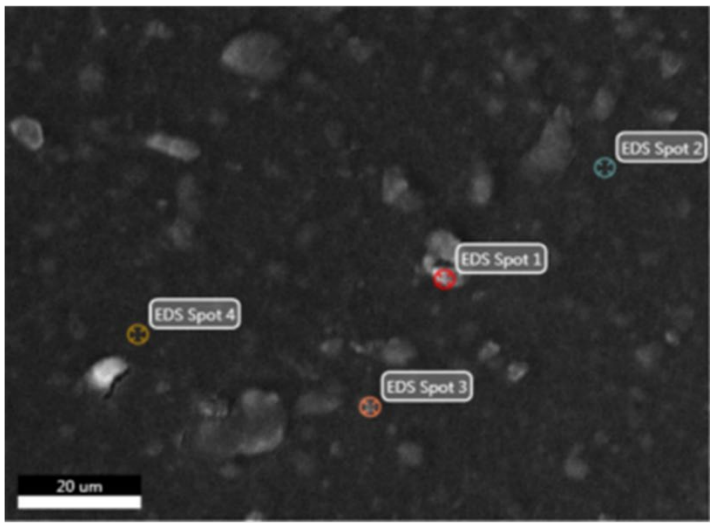

b

	Spot 1	Spot 2	Spot 3	Spot 4
Element	Atomic %	Atomic %	Atomic %	Atomic %
C K	52.03	46	52.05	52.94
O K	22.31	11.74	13.88	11.67
Si K	23.82	41.03	32.53	34.22
Cl K	0.39	0.29	0.36	0.27
K K	0.2	0.18	0.23	0.2
Cr K	1.25	0.76	0.95	0.7

Figure S21. **(a)** SEM scan of DAVG-PDI at 2.86kx magnification, **(b)** quantitative elemental composition analysis by SEM of EDS spots identified in (c), **(c)** EDS scans from SEM for spots 1, 2, 3, and 4.

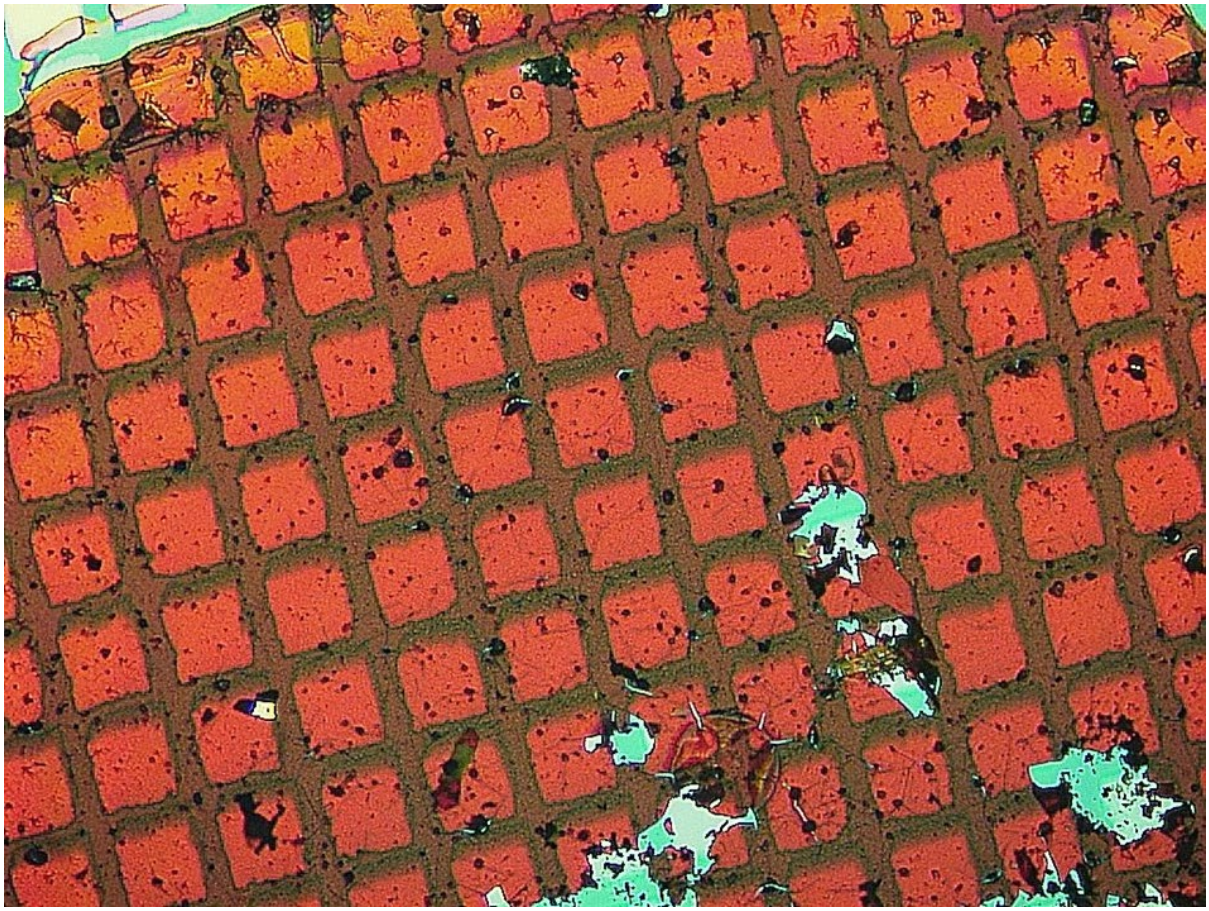

Figure S22. Representative image of VEVAA-PDI showing brittleness of π-peptides with alanine amino acid closest to the PDI cores resulting in thin films shattering upon contact with probe tip for electrical measurements.

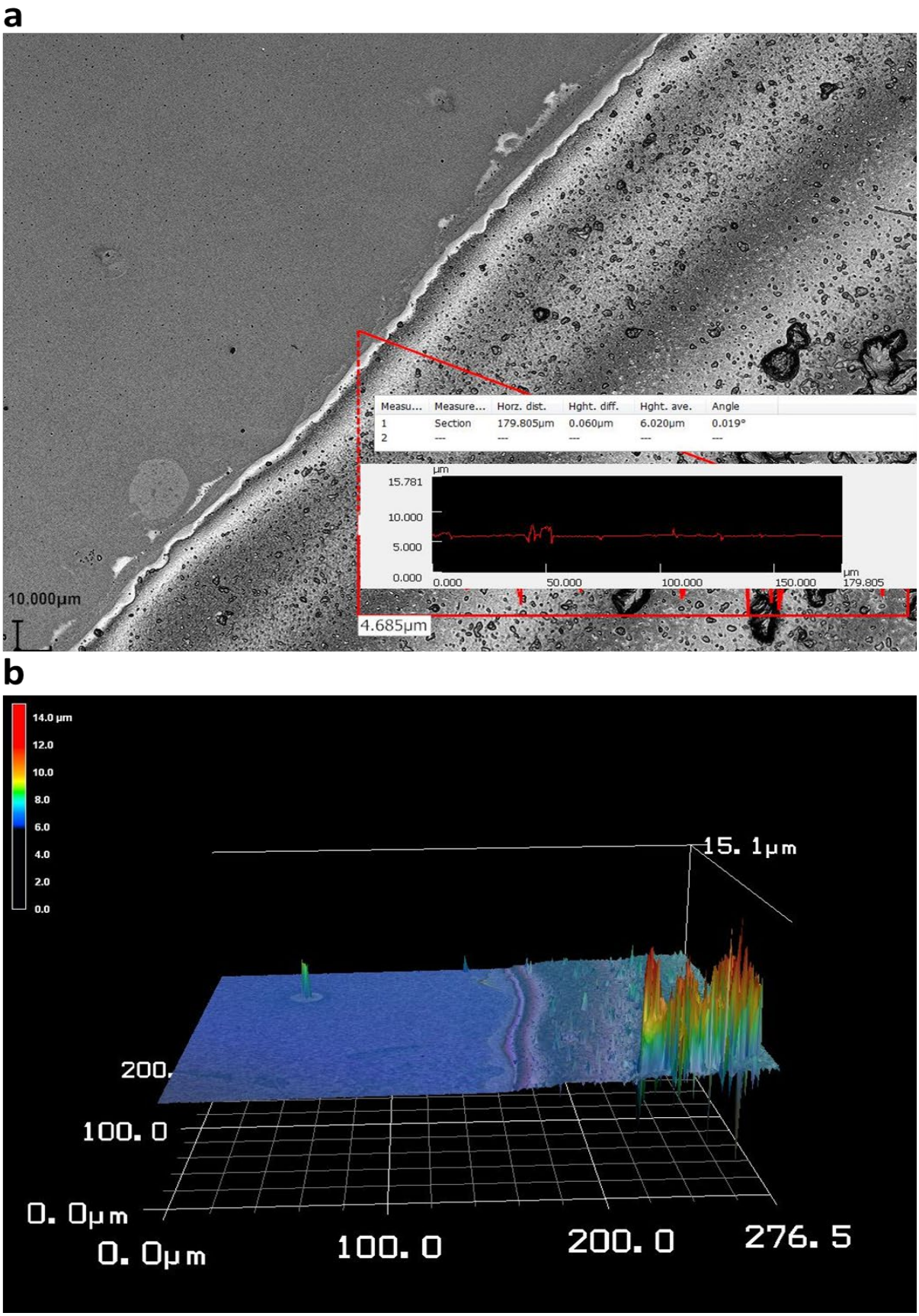

Figure S23. **(a)** Surface roughness profiling of laser scanned region at the edge of VEVAG-PDI thin film on Si substrate and **(b)** 3D height profile image of same area for thickness.

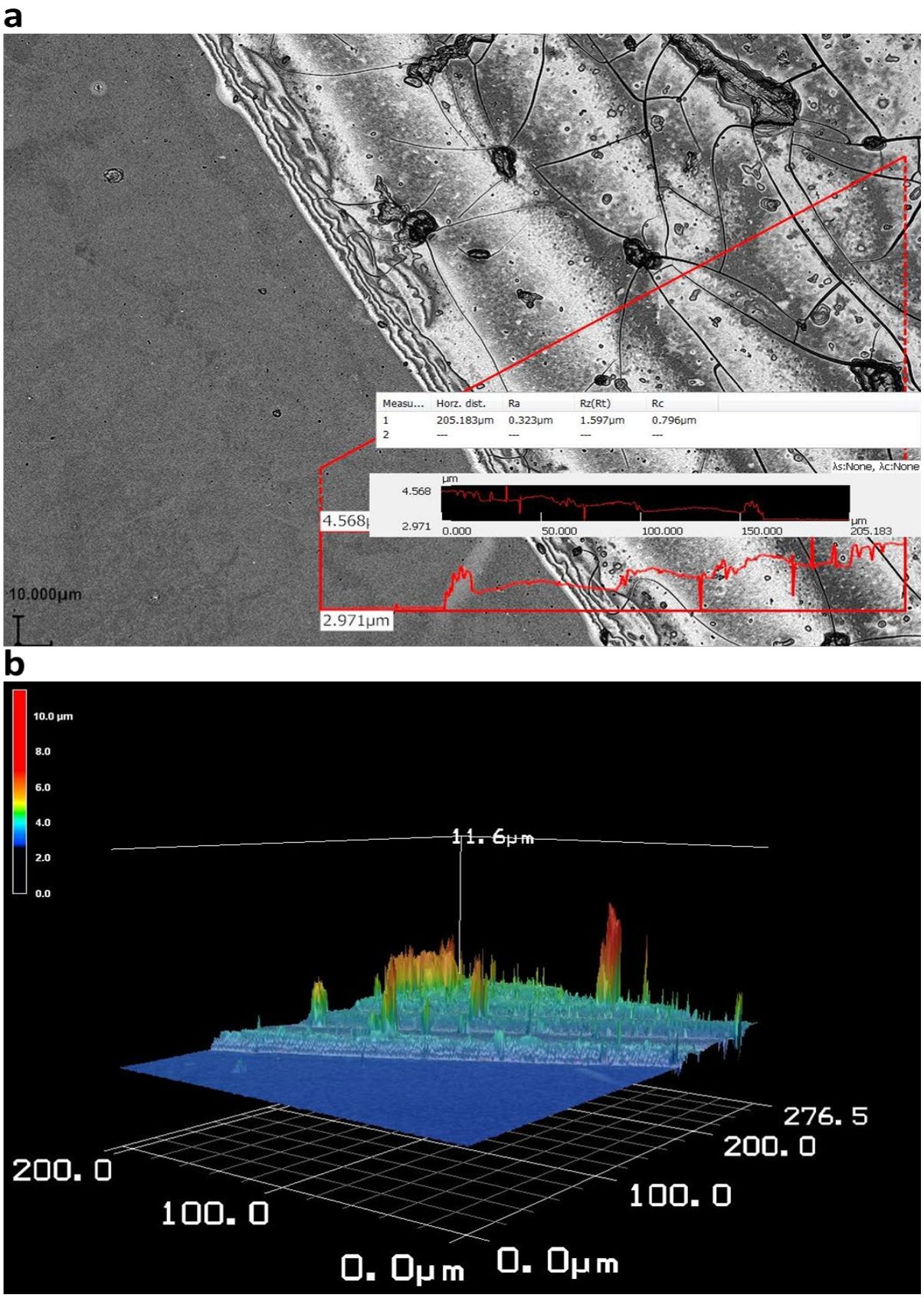

Figure S24. **(a)** Surface roughness profiling of laser scanned region at the edge of VEVAA-PDI thin film on Si substrate and **(b)** 3D height profile image of same area for thickness.

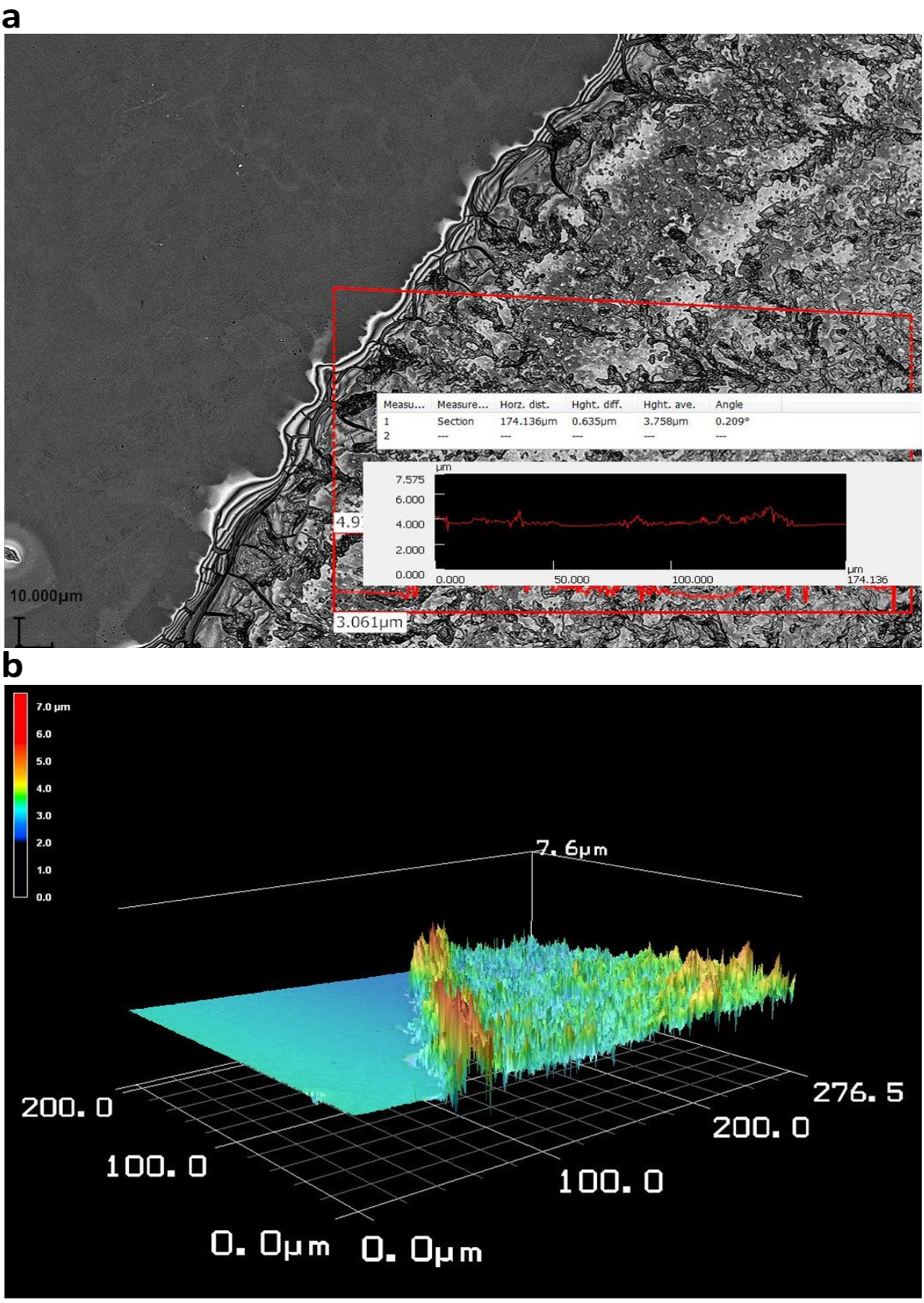

Figure S25. **(a)** Surface roughness profiling of laser scanned region at the edge of DAVG-PDI thin film on Si substrate and **(b)** 3D height profile image of same area for thickness.

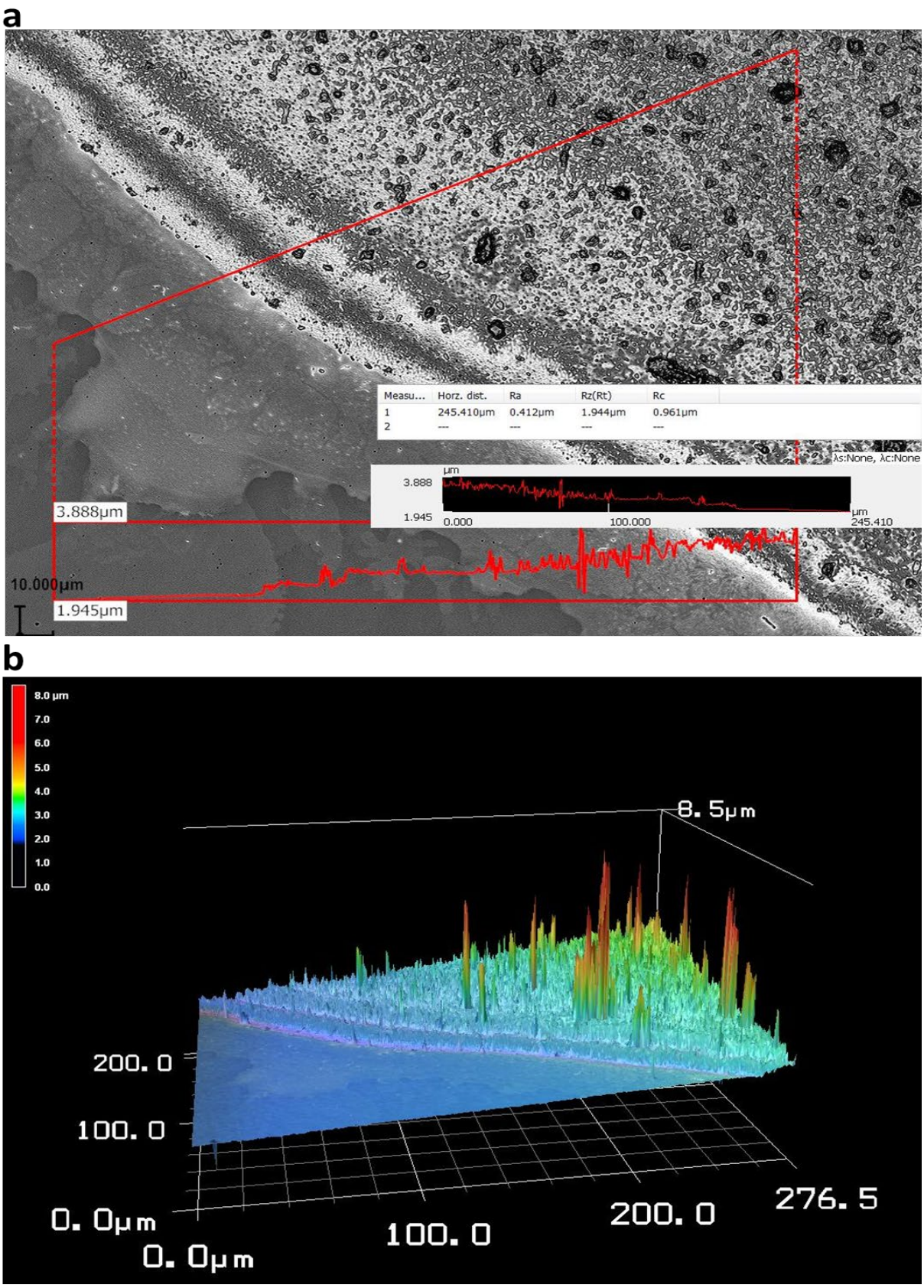

Figure S26. **(a)** Surface roughness profiling of laser scanned region at the edge of DAIA-PDI thin film on Si substrate and **(b)** 3D height profile image of same area for thickness.